Flow coherent structures and frequency signature: application of the dynamic modes decomposition to open cavity flow

2011 J. Phys.: Conf. Ser. 318 042036

(http://iopscience.iop.org/1742-6596/318/4/042036)

Journal of Physics: Conference Series **318** (2011) 042036 doi:10.1088/1742-6596/318/4/042036

Flow coherent structures and frequency signature: application of the dynamic modes decomposition to open cavity flow

F. Lusseyran[1],F. Guéniat[1,2], J. Basley[1,2,5], C. L.Douay[1,3], L. R. Pastur[1,2], T. M. Faure [1,3] & P.J. Schmid[4]

[1]LIMSI-CNRS BP 133, F-91403 Orsay Cedex, France,
[2]Univeristé Paris Sud 11, F-91405 Orsay Cedex, France,
[3]Université Pierre & Marie Curie, 4 place Jussieu, F-75252 Paris Cedex 05, France,
[4]LadHyX, Ecole Polytechnique, F-91128 Palaiseau, France
[5]LTRAC, Department of Aerospace and Mechanical Engineering, Monash University, Melbourne VIC 3800, Australia

Abstract. The dynamic dimension of an impinging flow may be significantly reduced by its boundary conditions and self-sustained oscillations they induce. The spectral signature is associated with remarkable spatial coherent structures. Dynamic modes decomposition (DMD) makes it possible to directly extract the dynamical properties of a non-linearly saturated flow. We apply DMD to highlight the spectral contribution of the longitudinal and transverse structures of an experimental open-cavity flow.

1. Introduction

Although open physical systems potentially have an infinite number of degrees of freedom, flows quite often organize around characteristic coherent structures, which play a key-role in both the dynamics and spectral signature of the flow (e.g. von Karman streets or self-sustained oscillating flows). This organization invites a modal decomposition which can be used to understand the connection between the different scales captured by the coherent structures and their time behavior, or to infer reduced-order models. Classical decompositions are Fourier, proper orthogonal decomposition (POD), or global mode decompositions. POD is based on a statistical correlation and can therefore be applied to experimental data, while global modes rely on some linearized evolution operator and are therefore not easy to deal with experimentally. Dynamic mode decomposition (DMD) is based on the analysis of the Koopman operator [1] and aims at extracting the non-linear dynamical features of the flow [2; 3; 4] from time-resolved experimental data. In this contribution we consider the case of an experimental open-cavity flow, in the incompressible regime, from which velocity fields were computed using time-resolved particle image velocimetry (TR-PIV). The spectral signature of the longitudinal spatial structures, obtained using DMD, will be compared to the signature obtained by discrete Fourier transform, yielding a validation. DMD modes of the transversal spatial structures allow the difficult identification of the spectral signature of the centrifugal instability inside the cavity (Görtler-like spanwise vortex).

2. Decomposition Method

DMD is a model-free algorithm yielding a decomposition of experimental flow fields into coherent and dynamically relevant structures [2; 3; 4]. Its underlying premise rests on the identification of a linear inter-snapshot mapping that best (in a least-squares sense) represents data produced by a non-linear process. The linear mapping can then be analyzed using eigenvalue-analysis, resulting in dominant frequencies and modal shapes. Considering a data set V_0^{N-1} of N realizations of the velocity field fluctuations, an evolution operator A is supposed, so that,

$$V_0^{N-1} = \{\boldsymbol{u}_0, \boldsymbol{u}_1, \ldots, \boldsymbol{u}_{N-1}\} = \{\boldsymbol{u}_0, A\boldsymbol{u}_0, \ldots, A\boldsymbol{u}_{N-2}\}\,. \tag{1}$$

Operator A describes the time development of the observable $\boldsymbol{u}$ resulting from a nonlinear process. The eigenfunctions ϕ_i of A and the eigenvalues λ_i, with $A\phi_i = \lambda_i\phi_i$, are therefore characteristic of the time behavior of the field $\boldsymbol{u}$. The set $\{\phi_i\}$ is infinite and builds a basis for the temporal evolution of the velocity field realizations,

$$\boldsymbol{u}(\boldsymbol{r}, t) = \sum_{i\geq 1} \phi_i(t)\boldsymbol{\alpha}_i(\boldsymbol{r}), \tag{2}$$

with $\boldsymbol{\alpha}_i$ as the projection of $\boldsymbol{u}$ onto $\{\phi_i\}$. The coefficients $\boldsymbol{\alpha}_i$ constitute the dynamical modes. Let us remark that, using equation (1), expression (2) can be written through a temporal recurrence:

$$\boldsymbol{u}(\boldsymbol{r}, t_k) = \sum_{i\geq 1} \lambda_i^{k-1}\phi_i(t_0)\boldsymbol{\alpha}_i(\boldsymbol{r}). \tag{3}$$

The computation of $(\phi_i, \boldsymbol{\alpha}_i)$ is accomplished under the assumption that the field $\boldsymbol{u}_N$ can be written as a linear combination of the flow realizations V_0^{N-1} :

$$\boldsymbol{u}_N = c_0\boldsymbol{u}_0 + c_1\boldsymbol{u}_1 + \ldots + c_{N-1}\boldsymbol{u}_{N-1}. \tag{4}$$

It follows from (1) that $AV_0^{N-1} = V_1^N$ which leads, with assumption (4), to the definition of the companion matrix C, according to $AV_0^{N-1} = V_0^{N-1}C + R$, with

$$C = \begin{pmatrix} 0 & \ldots & \ldots & 0 & c_0 \\ 1 & 0 & & \vdots & c_1 \\ 0 & 1 & \ddots & \vdots & c_2 \\ \vdots & \ddots & \ddots & 0 & \vdots \\ 0 & \ldots & 0 & 1 & c_{N-1} \end{pmatrix}, \tag{5}$$

and R denoting a residual matrix which is zero when (4) is strictly realized. The dimension of matrix C is $N \times N$ and the coefficients c_j are deduced from equation (4) by minimizing the norm of the difference vector $\boldsymbol{u}_N - \sum_{j=1}^{N-1} c_j\boldsymbol{u}_j$. The operators A and C are similar in the sense that, if the residual R is zero, they share the same eigenvalues; their eigenvectors are related via $\boldsymbol{\alpha}_j \simeq V_0^{N-1}\boldsymbol{v}_j$. An empirical estimation of the eigenvectors $\{\phi_i\}$ of the evolution operator A is therefore possible, leading to the equation:

$$\tilde{\boldsymbol{u}}_k = \sum_{i=1}^{N} \lambda_i^{k-1}\phi_i(t_0)\boldsymbol{\alpha}_i(\boldsymbol{r}). \tag{6}$$

The initial conditions $\{\phi_i(t_0)\}$ are obtained by projecting $\boldsymbol{u}_0$ onto $\{\boldsymbol{\alpha}_i\}$. For data sampled from a periodic dynamic process, dynamic modes have been shown to reduce to Discrete Fourier Transform (DFT) modes. It can be verified that this property remains valid for dynamics confined to an attractor, as recalled in [3] (and c.f. end of §4.1).

3. Experimental conditions

An open rectangular cavity is inserted in a wind flow tunnel. The airflow is generated by a centrifugal fan placed upstream of a settling chamber (Figure 1). The incoming airflow is laminar and stationary, and the flow rate is kept constant during the experiment. Between the external flow and the inside-cavity flow, a convectively unstable shear layer develops (Fig. 2a). The impact at the downstream cavity edge leads to self-sustained oscillations, which induce the main features in the power spectrum (Fig. 3 b). Besides this shear instability, the curvature of the recirculating flow inside the cavity (Fig. 2a) induces centrifugal instabilities over a given range of the control parameters U, L/H et S/H. In the saturated nonlinear regime this gives rise to near-toroidal Taylor-Görtler structures [5; 6] (see figure 2 b).

Two- or three-component velocity fields are obtained by particle image velocimetry using an optical flow algorithm applied to images pairs taken in the considered illuminated plane. As a reference, a local well-sampled time-series of the axial velocity component is recorded at one point of the flow by a laser Doppler velocimeter. The matching between a given frequency and the corresponding longitudinal or spanwise flow structure is performed using two different data bases, one corresponding to PIV measurements in the longitudinal plane $\{x, y, z = 0.07H\}$ near the plane of symmetry of the cavity, the other in the spanwise plane $\{z, x, y = -0.3H\}$. The parameters of the two databases are given in the following sections 4.1 and 4.2.

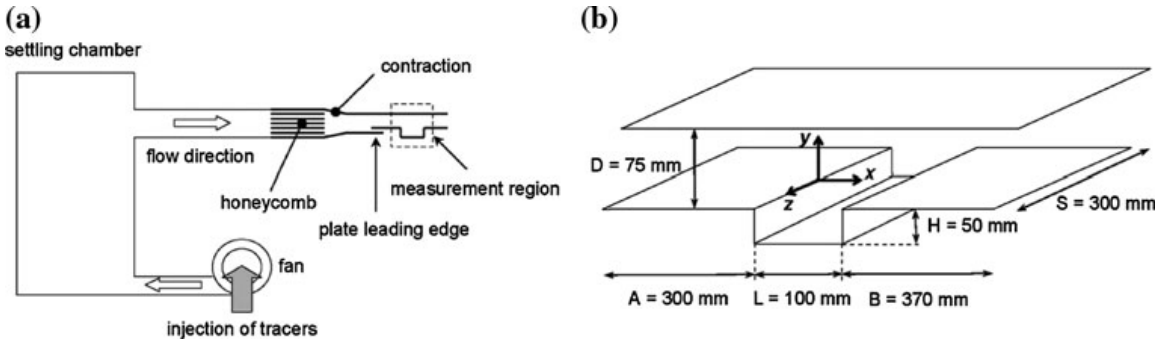

Figure 1. Sketch of the experimental setup, (a) windtunnel, (b) cavity sub-system with $L/H = 2$.

(a) (b)

Figure 2. Smoke visualization for a cavity geometry $L/H = 1.5$, $S/H = 6$ and for a typical Reynolds number $\Re_H \approx 3000$. (a) Front view of the longitudinal plane (x, y), (b) top view of the spanwise plane (x, z) located at $y/H = -0.3$ inside the cavity.

4. Dynamic Mode Decomposition of the cavity flow

4.1. Snapshot DMD in the longitudinal plane $\{x, y, z \approx 0\}$

For the study in the longitudinal plane the cavity geometry is chosen so that the ratio of length to height is $L/H = 2$ with $L = 100$ mm and $H = 50$ mm. The upstream velocity $U = 1.9$ m/s corresponds to the Reynolds numbers $\Re_L = UL/\nu_{air} = 12700$ and $\Re_H = UH/\nu_{air} = 6350$. A record of 8192 images (512x400 pixels) acquired with a high rate PIV system provides a series of 4092 velocity fields sampled at $250Hz$.

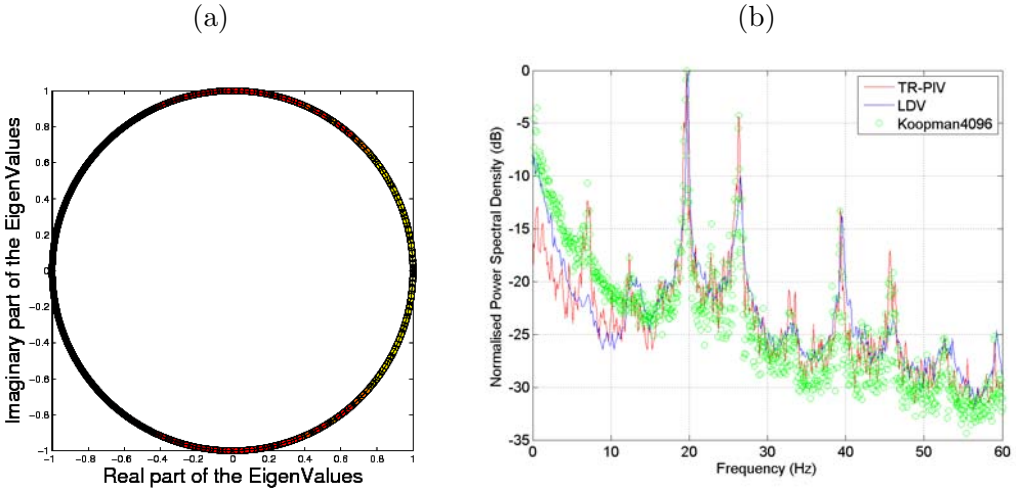

Figure 3. DMD of velocity fields in the longitudinal plane: (a) operator eigenvalues λ_k, well distributed on the unit circle. (b) Comparison between PSD obtained by Fourier transform of the LDV signal (solid blue line), amplitude spectrum of the DMD (green circles) and the mean value over space of the Fourier transform of the PIV snapshots (solid red line).

In thae nonlinearly saturated flow regime, the eigenvalues λ_k of the Koopman operator are distributed on the unit circle, as presented in figure 3a; they can therefore be written as $\lambda_k = \exp(i\omega_k \Delta t)$ and correspond to the frequencies $f_k = \omega_k/2\pi$. One can then determine an amplitude spectrum of the DMD modes, attributing to each frequency $f_k \pm \delta f_k/2$ an amplitude given by the L_2-norm of the corresponding mode $\boldsymbol{\alpha}_k$. This yields the spectrum shown in figure 3b (green circles) which appears to be similar to the PSD computed by the Fourier transform of the LDV time-series(solid blue line). The discrepancies can be partially attributed to the fact that the amplitude spectrum of the DMD modes reflects the behavior of the entire two-component velocity fields, whereas the PSD of the LDV-record of the axial-velocity component is strictly local. To estimate the difference between the global and the local behavior one can take the data set used for the DMD analysis and compute the Fourier transform of each local time series. These local PSDs are then averaged over space (see figure 3b, solid red line). The agreement with the spectrum of the DMD modes (green circles) is very good, both in frequency and amplitude, at least for the main peaks associated with the shear layer instability.

The spatial structures $\boldsymbol{\alpha}_k$, associated with the frequencies f_k which are most prominent in the spectrum of the figure 3b, are given in figure 4. As expected, the high, dominant frequencies correspond to oscillatory modes of the shear layer (figure 4 c and d), while low frequencies correspond to structures inside the cavity (figures 4 a and b). These DMD modes are compared to those obtained by a direct projection of the matrix V_0^{N-1} onto Fourier modes using a discrete Fourier transform (DFT) as presented in detail by Basley et al. [7]. The real part of the DFT modes is plotted in figure 4 d,e,f and g for the same four frequencies than detected by the

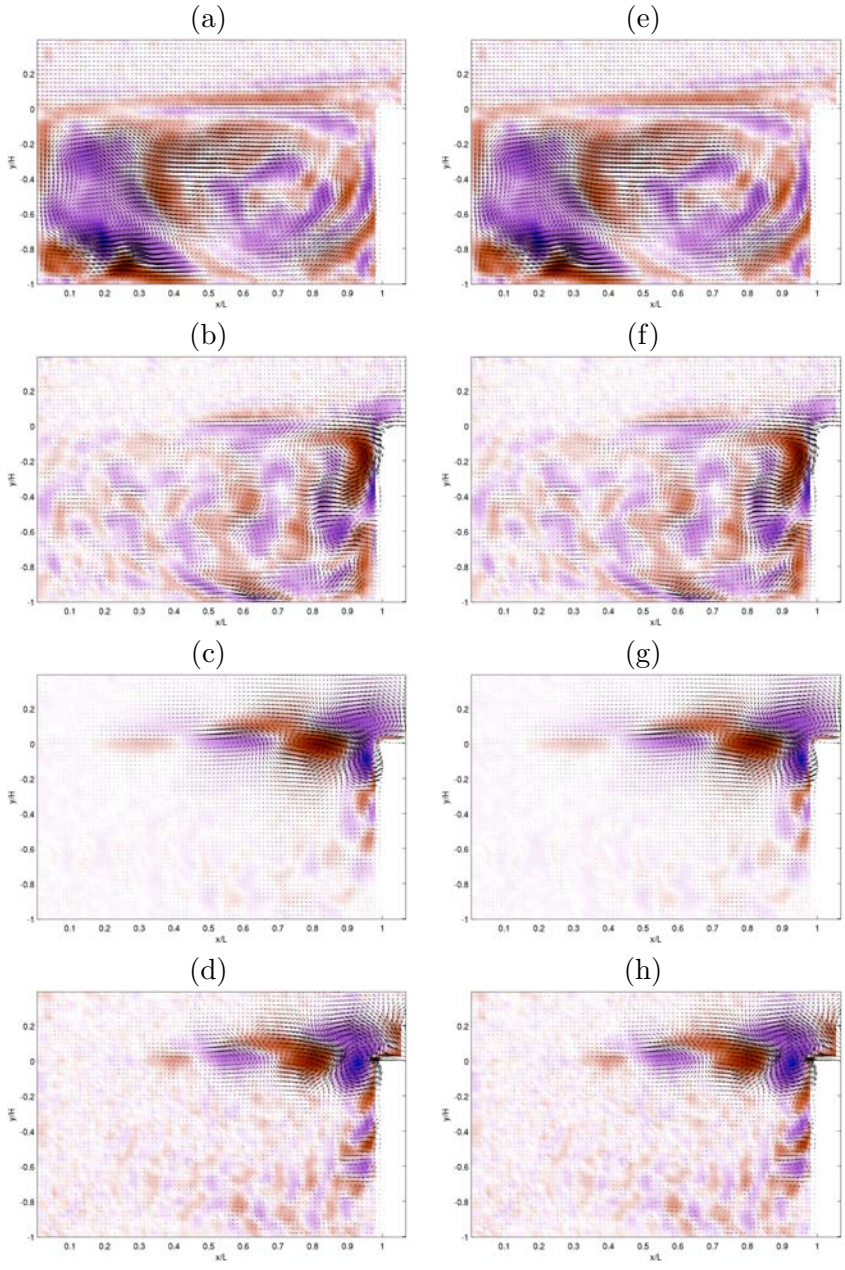

Figure 4.
DMD modes (left column)
DFT Modes (right column)
Inside cavity structures:
(a) & (e) $f_k = 0.49$ Hz,
(b) & (f) f_k =7.1 Hz,
Mixing layer structures:
(c) & (g) f_k =19.6 Hz,
(d) & (h) $f_k = 26.4$ Hz,

Quiver field shows the real part of $\boldsymbol{\alpha}_k = \alpha_{k,x}\boldsymbol{e}_x + \alpha_{k,y}\boldsymbol{e}_y$ and the colorbar shows the normalized vorticity intensity.

DMD analysis. The two methods give indeed extremely close results. Because DFT and DMD modes are complex, a comparison of both of them require to find empirically the common phase. Although remarkable from the point of view of the numerical precision,this similarity between both methods is expected since Koopman eigenvalues λ_k are close to complex exponential functions (as observed in Figure 3a), hence describe purely oscillating dynamics. Indeed, a permanent regime, that is a system evolving on an attractor, implies by definition oscillating modes without any growth rate (no transitory component): DMD modes of a permanent regime tend to global Fourier modes as analytically demonstrated in [3] in the case of a discrete system of finite dimension.

4.2. Snapshot DMD in the spanwise plane $\{x, z, y = -0.3H\}$

For a frequency characterization of the spanwise flow structures, the cavity geometry is chosen such that the ratio of length-to-height is $L/H = 1.5$ with $L = 75$ mm and $H = 50$ mm (Fig. 1). The upstream velocity $U = 0.69$ m/s corresponds to the Reynolds numbers $\Re_L = UL/\nu_{air} = 3066$ and $\Re_H = UH/\nu_{air} = 2300$. A record of 2000 images (with 1032x732 pixels) gives, after computation of the particle displacements, a series of 1000 velocity fields sampled at $5Hz$.

Görtler-like vortices are moving towards the cavity sides due to Ekman-layer pumping. The point of separation, between the two directions, occurs off-center at $z_c/S = 0.067$. To save RAM, only a limited area of 500×200 pixels (138×51 mm^2) centered around z_c is concidered and DMD modes associated with the velocity components u_x et u_z are computed separately.

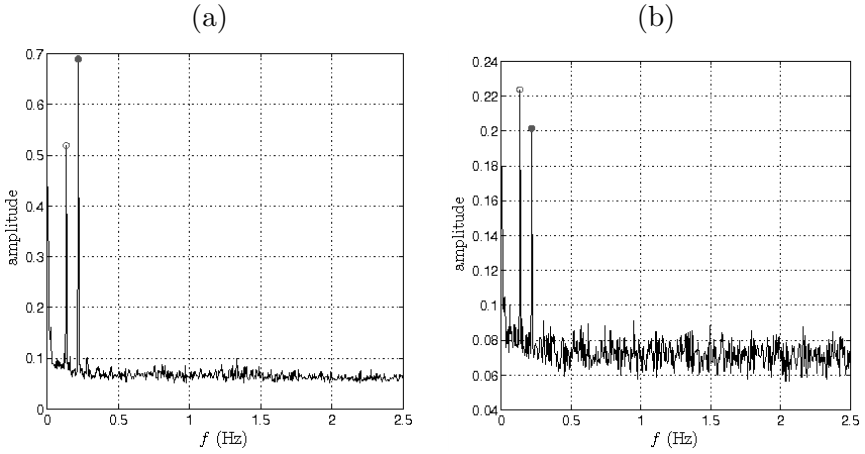

Figure 5. Spectrum associated with the DMD $\boldsymbol{\alpha}_k$ of the spanwise dataset
(a) $\{u_x\}$,
(b) $\{u_z\}$.

The eigenvalues for both the $\{u_x\}$- and $\{u_z\}$-modes are again closely distributed on the unit circle, indicating that the data series is sufficiently long. The amplitude spectrum of the spanwise DMD modes (figure 5) presents clearly three main frequencies, $f_1 = 0.13$ Hz (open circle), $f_2 = 0.22$ Hz (solid circle) and a very low one $f_3 = 0.005$ Hz. Between the $\{u_x\}$- and $\{u_z\}$-analysis, only the amplitude is changing; the identified frequencies are the same. The corresponding eigenvectors $\boldsymbol{\alpha}_1$ and $\boldsymbol{\alpha}_2$ associated with f_1 and f_2 are given in figure 6. They signify a link between the detected frequencies and a centrifugal instability for two reasons. First, they express the slow motion induced by the Ekman-layer pumping, left for $\boldsymbol{\alpha}_1$ and right for $\boldsymbol{\alpha}_2$; indeed, imaginary and real parts are mainly in phase quadrature. The expression $\boldsymbol{\alpha}_1(\boldsymbol{r}) \simeq \boldsymbol{\alpha}_{1,r}(x, z) + i\boldsymbol{\alpha}_{1,r}(x, z + \lambda_1/4)$, when multiplied by the temporal coefficient $\phi_1(t) = e^{2i\pi f_1 t}$, gives the dynamics of a convective wave moving left,

$$\tilde{\boldsymbol{u}}_1(\boldsymbol{r}, t) = (\phi_1(t)\boldsymbol{\alpha}_1(\boldsymbol{r}) + \text{c.c.})/2 = \boldsymbol{\alpha}_{1,r}(x, z)\cos(\omega_1 t) - \boldsymbol{\alpha}_{1,r}(x, z + \lambda_1/4)\sin(\omega_1 t),$$

while the analogous expression with $\boldsymbol{\alpha}_2$ represents a right-moving vortices. This relation is confirmed by a movie based on the time-series reconstruction. Secondly, the quiver representation of $\boldsymbol{\alpha}_1$ and $\boldsymbol{\alpha}_2$ exhibits vortices at both the down- and upstream ends where Görtler votices are present.

5. Conclusions

Dynamics in an open cavity mainly comes down to a few spectral components which have been long studied, questions remains as for a refined analysis of modulation processes and various 3D-instabilities implied by internal flow. The system is characterized by time scales over two orders of magnitude corresponding to a full three-dimensional evolution of coherent flow structures.

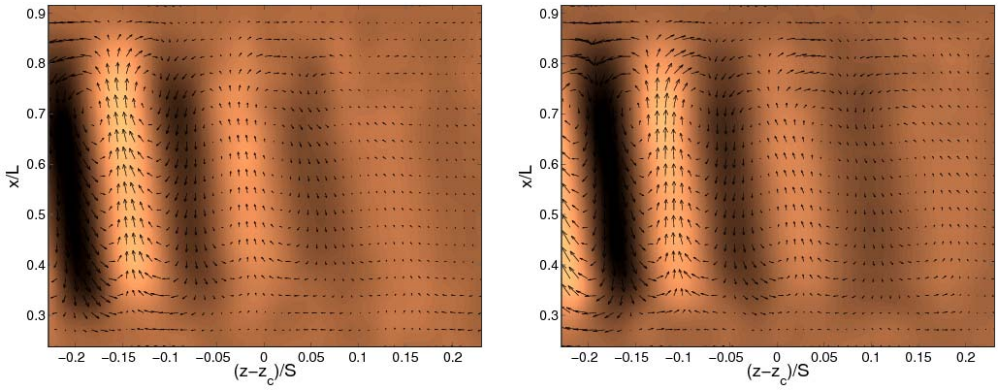

(a) $\Re(\boldsymbol{\alpha}_1)$ (b) $\Im(\boldsymbol{\alpha}_1)$

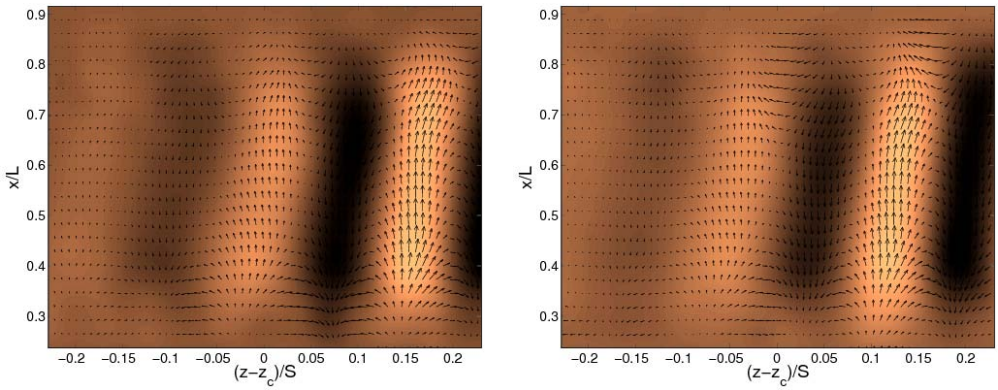

(c) $\Re(\boldsymbol{\alpha}_2)$ (d) $\Im(\boldsymbol{\alpha}_2)$

Figure 6. Real and imaginary parts of vectors $\boldsymbol{\alpha}_1$ and $\boldsymbol{\alpha}_2$, associated with $f_1 = 0.13$ Hz and $f_2 = 0.22$ Hz. Quivers give the real part (α_z, α_x), and color contours represent the real part of $\boldsymbol{\alpha}_k \cdot \boldsymbol{e}_x$.

We capture the dynamical range over these time scales using the dynamic mode decomposition, which provides a good numerical estimation of the modes of Koopman evolution operator, from the experimental data set. This decomposition requires a time-resolved dataset. For this reason, two different flow configurations and three kinds of velocimetries are used in this study. We show that, in such a flow, the DMD can reveal a connection between a frequency and some space-time behavior of the corresponding structures. Dynamic decomposition is first employed in the plane perpendicular to the shear layer in order to catch the primary instability, which induces self-sustained oscillations impinging the trailing edge of the cavity the most energetic instabilities develop in the shear layer (§4.1). It is then applied to analyze the Taylor-Görtler-like structures in the orthogonal spanwise plane (§4.2). The two main frequencies corresponding to self-sustained oscillations inside the shear layer 19.6 Hz and 26.4 Hz are well separated. Such a separation cannot be obtained using the proper orthogonal decomposition (POD). In particular, two of these spectral components denote in fact a progressive wave as a spanwise mode slowly drifting towards the Eckman layers located at the transversal walls of the cavity. In the transverse plane, two frequencies have been identified and linked to the unsteady behavior of Görtler-like spanwise structures. In particular, two of these spectral components denote in fact a progressive wave: a spanwise mode slowly drifting towards the Eckman layers located at the transversal walls of the cavity.

References

[1] B.O. Koopman, Hamiltonian systems and transformations in Hilbert space, *Proceedings of the National Academy of Sciences* **17**, pp 315-318 (1931).

[2] P.J. Schmid and J. Sesterhenn, *Sixty-First Annual Meeting of the APS Division of Fluid Dynamics*, San Antonio, Texas, USA (2008).

[3] C. Rowley et al., *J. Fluid Mech.* **641**:115–127, 2009.

[4] P.J. Schmid, *J. Fluid Mech.* **656**:5–28, 2010.

[5] T.M. Faure et al., *Experiments in Fluids*, **42-2**:169 184 (2007).

[6] T.M. Faure et al., *Experiments in Fluids*, **47-3**:395-410 (2009).

[7] J. Basley, L. R. Pastur, F. Lusseyran, T. M. Faure, N. Delprat, Experimental investigation of global structures in an incompressible cavity flow using time-resolved PIV, *Experiments in Fluids* (2010), 50:905-918